

# FastInsight: Fast and Insightful Retrieval via Fusion Operators for Graph RAG

Seonho An  
KAIST  
Daejeon, Republic of Korea  
asho1@kaist.ac.kr

Chaejeong Hyun  
KAIST  
Daejeon, Republic of Korea  
hchaejeong@kaist.ac.kr

Min-Soo Kim\*  
KAIST  
Daejeon, Republic of Korea  
minsoo.k@kaist.ac.kr

## Abstract

Existing Graph RAG methods for insightful retrieval on corpus graphs typically rely on time-intensive processes that interleave LLM reasoning. To enable time-efficient insightful retrieval, we propose **FastInsight**. We first introduce a graph retrieval taxonomy that categorizes existing methods into three fundamental operations: vector search, graph search, and model-based search. Through this taxonomy, we identify two critical limitations: topology-blindness in model-based search and semantics-blindness in graph search. FastInsight overcomes these limitations by interleaving two novel fusion operators: the **Graph-based Reranker (GRanker)**, which acts as a graph model-based search, and **Semantic-Topological eXpansion (STeX)**, which serves as a vector-graph search. Extensive experiments on broad retrieval and generation datasets demonstrate that FastInsight significantly improves both retrieval accuracy and generation quality compared to state-of-the-art baselines, while achieving significant Pareto improvements in the trade-off between effectiveness and efficiency. Our code is available at this [Anonymous GitHub Link](#).

## CCS Concepts

- Information systems → Retrieval models and ranking; Language models; Rank aggregation;
- Computing methodologies → Knowledge representation and reasoning.

## Keywords

Retrieval-Augmented Generation, Graph Retrieval, Reranking

### ACM Reference Format:

Seonho An, Chaejeong Hyun, and Min-Soo Kim. 2026. FastInsight: Fast and Insightful Retrieval via Fusion Operators for Graph RAG. In *Proceedings of Make sure to enter the correct conference title from your rights confirmation email (SIGIR'26)*. ACM, New York, NY, USA, 11 pages. <https://doi.org/XXXXXX.XXXXXXX>

\*Corresponding author.

Permission to make digital or hard copies of all or part of this work for personal or classroom use is granted without fee provided that copies are not made or distributed for profit or commercial advantage and that copies bear this notice and the full citation on the first page. Copyrights for components of this work owned by others than the author(s) must be honored. Abstracting with credit is permitted. To copy otherwise, or republish, to post on servers or to redistribute to lists, requires prior specific permission and/or a fee. Request permissions from [permissions@acm.org](mailto:permissions@acm.org).

SIGIR'26, Woodstock, NY

© 2026 Copyright held by the owner/author(s). Publication rights licensed to ACM. ACM ISBN 978-1-4503-XXXX-X/2026/06  
<https://doi.org/XXXXXX.XXXXXXX>

## 1 Introduction

Retrieval-Augmented Generation (RAG) has emerged as a widespread solution to mitigate the inherent limitations of Large Language Models (LLMs), such as hallucinations and outdated parametric knowledge [13]. However, RAG methods that rely on vector search (referred to as Vector RAG) inherently fail to capture structural dependencies and non-textual information, such as reference networks between documents, due to their reliance on its vector database [10, 15, 17, 42]. To address this, recent studies have proposed **Graph RAG** methods [7, 15, 17, 21, 25, 30, 37, 42], which incorporate a *graph* structure into the retrieval process to capture relationships via edges [18].

Recently, increasing attention has been paid to *corpus graphs*—such as reference networks [1]—in which each node contains rich textual information [7, 16, 31, 34]. Unlike conventional knowledge graphs (KGs), nodes in corpus graphs generally encapsulate explicit clues to guide the retrieval process. Thus, Graph RAG methods on corpus graphs require strong capabilities for **Insightful Retrieval**—defined as an iterative process of (**P1**) understanding the intermediate retrieval results, and (**P2**) deciding a new retrieval based on understanding [3, 23, 27, 39].

Conventional approaches have implemented this process through retrieval-generation interleaving methods that leverage the strong reasoning capabilities of LLMs [27, 30, 37, 39]. However, such methods incur prohibitively high latency, often reaching up to tens of seconds [9, 36]. From a human-computer interaction (HCI) perspective, these delays significantly degrade user satisfaction [5, 26], thereby hindering the practical adoption of such solutions in enterprise environments.

Accordingly, this paper aims to propose a *time-efficient and effective* graph retrieval method for Graph RAG that can directly perform insightful retrieval while meeting real-time demands. To design such an insightful retriever, it is first necessary to systematically decompose and understand the operational mechanisms of graph retrieval employed in existing Graph RAG methods. To this end, we propose a **graph retrieval taxonomy** that categorizes graph retrieval algorithms as combinations of three fundamental retrieval operations: Vector Search ( $O_{vs}$ ), Graph Search ( $O_{gs}$ ), and Model-based search ( $O_m$ ). Specifically,  $O_{vs}$  retrieves nodes based on semantic vector indices (e.g., dense passage retrieval),  $O_{gs}$  traverses the graph relying solely on graph topology (e.g., one-hop traversal), and  $O_m$  represents discriminative scoring models (e.g., Cross-Encoders or lightweight SLMs) that evaluate the semantic relevance of a node.

For instance, Figure 1 illustrates an example query about Agentic RAG components and the corresponding retrieval behaviors of three representative graph retrieval methods: (b) LightRAG [15],

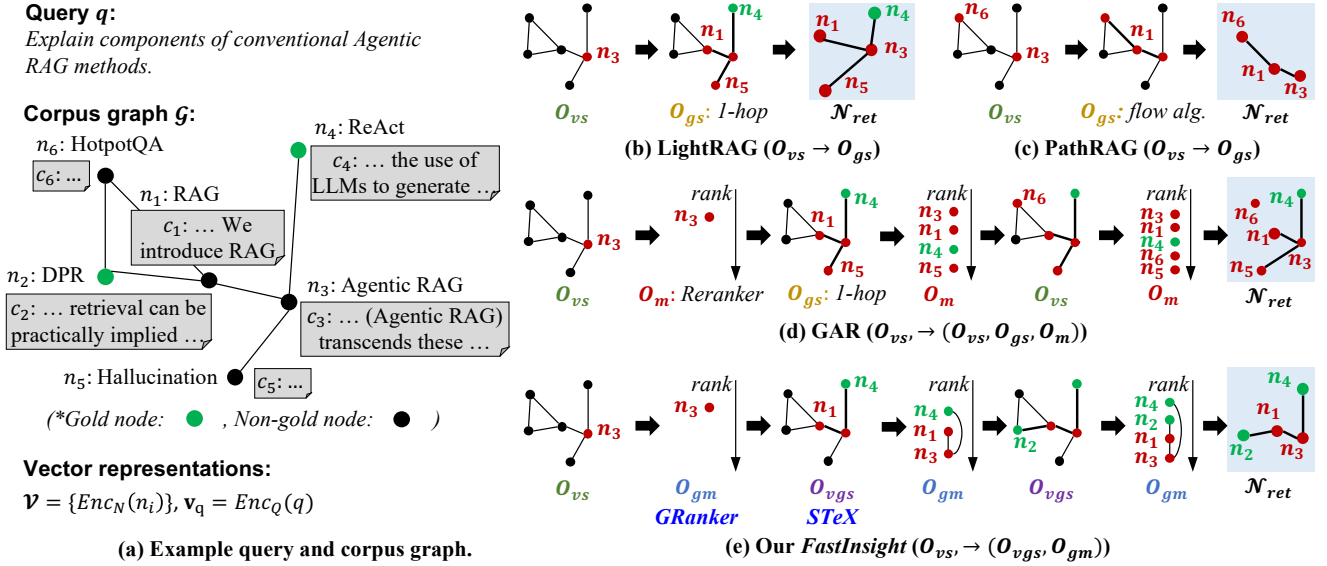


Figure 1: Conceptual comparison of graph retrieval workflows based on retrieval operations. (a) illustrates the inputs for graph retrieval:  $q$ ,  $\mathcal{G}$ ,  $v_q$  and  $\mathcal{V}$ . (b)–(d) depict representative graph retrieval methods, while (e) presents our *FastInsight* method.

(c) PathRAG [7], and (d) GAR [31]. Specifically, LightRAG follows a sequence of  $O_{vs}$  and  $O_{gs}$  (i.e.,  $O_{vs} \rightarrow O_{gs}$ ). In contrast, as shown in Figure 1(d), GAR begins with  $O_{vs}$  and subsequently performs an interleaving of  $O_m$ ,  $O_{gs}$ , and  $O_{vs}$  (i.e.,  $O_{vs} \rightarrow (O_{vs}, O_{gs}, O_m)$ ). Based on these operator compositions, we categorize and summarize representative graph retrieval methods in Table 1.

Table 1: Comparison of representative Graph RAG methods based on target database and retrieval operators.

Target database	Methods	Basic operations			Fusion operators	
		$O_{vs}$	$O_{gs}$	$O_m$	$O_{vgs}$	$O_{gm}$
Knowledge graph	HyKE [24]	✓	✗	✗	✗	✗
	HippoRAG [25]					
	GNN-RAG [32]	✓	✓	✗	✗	✗
	G-Retriever [19]					
	SubgraphRAG [28]	✓	✗	✓	✗	✗
	LightPROF [2]	✓	✓	✓	✗	✗
Corpus graph	ToG [37]	✓	✓	✓	✗	✗
	LightRAG [15]	✓	✓	✗	✗	✗
	PathRAG [7]	✓	✗	✗	✗	✗
Corpus graph + KG	GRAG [20]	✓	✗	✗	✗	✗
	KG2RAG [42]	✓	✓	✓	✗	✗
Documents + KG	ToG 2.0 [30]	✓	✓	✓	✗	✗
	HippoRAG 2 [17]	✓	✓	✗	✗	✗
Corpus graph	<b>FastInsight (ours)</b>	✓	-	-	✓	✓

However, implementing insightful retrieval using only the three operators employed in existing graph retrieval methods entails two inherent challenges: **(C1)** *topology-blindness* of  $O_m$ , and **(C2)** *semantics-blindness* of  $O_{gs}$ . First, regarding C1,  $O_m$  operators evaluate nodes solely based on textual content, ignoring topological context and thus failing to capture the contextual signals provided by neighboring nodes. For example, in Figure 1 (d), the second  $O_m$  operator correctly identifies that node  $n_4$  describes *a new prompting strategy for LLMs*; however, it fails to determine whether this is relevant to the *Agentic RAG methods* specified in  $q$  due to the lack of structural context. Second, regarding C2, while  $O_{vs}$  is inherently

static,  $O_{gs}$  relies exclusively on graph topology, often retrieving semantically irrelevant nodes. For example, in Figure 1 (d), the first  $O_{gs}$  operator traverses the graph toward node  $n_5$  (*Hallucination*) solely based on topological connectivity, despite its lack of semantic relevance to  $n_3$  (*Agentic RAG techniques*).

To address these two challenges, we propose (1) two novel advanced operators, **Graph Model-based Search** ( $O_{gm}$ ) and **Vector-Graph Search** ( $O_{vgs}$ ), that extend the basic operators, and (2) **FastInsight**, a fast and insightful graph retrieval method for corpus graphs that leverages these operators. Unlike basic graph retrieval operators, the proposed operators jointly exploit both topological and semantic information of input graphs to generate outputs.

Specifically, as the first realization of the  $O_{gm}$  operator, we propose the **Graph-based Reranker (GRanker)**. Treating topology-blind cross-encoder latent vector representations as noisy signals, GRanker applies a *first-order Laplacian approximation* to denoise these representations through structural aggregation. Furthermore, as the first realization of the  $O_{vgs}$  operator, we propose the **Semantic-Topological eXpansion (STeX)** algorithm. Given seed nodes and graph topology (for graph traversal), together with semantic vector indices and the query vector (for vector search), STeX performs graph search that dynamically incorporates vectorspace proximity during expansion.

Our FastInsight is defined as an iterative interleaving of the  $O_{gm}$  and  $O_{vgs}$  operators following the initial  $O_{vs}$  operation (i.e.,  $O_{vs} \rightarrow (O_{gm}, O_{vgs})$ ), as shown in Figure 1 (e). In this example, the proposed  $O_{gm}$  and  $O_{vgs}$  operators address Challenges 1 and 2, respectively, as follows: (1) the  $O_{gm}$  operator identifies that node  $n_4$  is relevant to *Agentic RAG* and consequently ranks  $n_4$  higher than  $n_3$ ; and (2) the  $O_{vgs}$  operator expands to node  $n_2$  (representing *DPR*) rather than the topologically equivalent node  $n_6$  (representing *HotpotQA*), since  $n_2$  exhibits higher vector similarity to the query.

To evaluate the effectiveness of FastInsight, we aim to answer the following three research questions (RQs):

#### Research Questions

- RQ1** Does **FastInsight** demonstrate superior retrieval accuracy and generation quality compared to state-of-the-art baselines on corpus graphs?
- RQ2** Is **FastInsight** significantly more time-efficient than existing graph retrievers, particularly compared to interleaving methods?
- RQ3** Does the performance improvement of **FastInsight** primarily stem from the realization of *insightful retrieval* that effectively exploits graph topology?

To answer these questions, we conduct both retrieval and generation experiments across two types of corpus graphs: **reference networks** [1, 35, 41] and **text-rich knowledge graphs** [7, 8, 10, 15]. The experimental results consistently provide affirmative answers to all three RQs. In particular, to address **RQ3** we propose a new retrieval metric, **Topological Recall**. Unlike standard Recall, which only measures whether oracle nodes are retrieved, Topological Recall additionally quantifies the *graph-theoretic proximity* between retrieved nodes and oracle nodes. This metric confirms that FastInsight not only retrieves relevant nodes but also effectively approaches oracle nodes in the graph. Our main contributions are summarized as follows:

- We propose a novel **graph retrieval taxonomy** that deconstructs existing graph retrieval methods into three operations:  $O_{\text{vs}}$ ,  $O_{\text{gs}}$ , and  $O_{\text{m}}$ , and identify two challenges: **topology-blindness of  $O_{\text{m}}$**  and **semantics-blindness of  $O_{\text{gs}}$** .
- We introduce two advanced fusion operators,  $O_{\text{gm}}$  and  $O_{\text{vgs}}$ , to address these two challenges. As their first realizations, we present the **Graph-based Reranker (GRanker)** and the **Semantic-Topological eXpansion (STeX)** algorithm, respectively.
- We propose **FastInsight**, a novel fast and effective graph retrieval method that integrates  $O_{\text{gm}}$  and  $O_{\text{vgs}}$ , demonstrating significant performance improvements across two types of corpus graph types while maintaining strong time efficiency.

## 2 Preliminaries

### 2.1 Graph RAG for Corpus Graphs

In this paper, we focus on *corpus graphs*, defined as follows:

**Definition 1** (Corpus Graph). A graph  $\mathcal{G} = (\mathcal{N}, \mathcal{E})$  is classified as a *corpus graph* if and only if every node  $n \in \mathcal{N}$  is associated with a pair  $(k_n, c_n)$ :  $k_n$  serves as a node identifier (key), and  $c_n$  provides descriptive textual information (textual content) about the node.

Graph RAG methods for *corpus graphs* take a query  $q$  and a corpus graph  $\mathcal{G} = (\mathcal{N}, \mathcal{E})$  as inputs, and generate an answer  $a$  through the following two steps:

- (1) **Graph Retrieval Step:** Given  $q$  and  $\mathcal{G} = (\mathcal{N}, \mathcal{E})$ , the objective is to retrieve a set of nodes  $\mathcal{N}_{\text{ret}} \subseteq \mathcal{N}$  that are *relevant* to  $q$ .
- (2) **Generation Step:** An answer  $a$  is generated based on  $q$  and the retrieved node contents  $C_{\text{ret}} = \{c_i \mid (k_i, c_i) \in \mathcal{N}_{\text{ret}}\}$

using a generative language model  $P_\theta$ . Conventionally,  $P_\theta$  processes  $q$  and  $C_{\text{ret}}$  via in-context learning.

Graph RAG methods operating on other graph types, such as social networks, fall outside the scope of this paper and are left for future work. While some variants of corpus graphs, such as text-rich knowledge graphs used in LightRAG [15], incorporate textual descriptions on edges [7, 15], this work does not explicitly focus on leveraging edge-level textual information.

## 2.2 Insightful Retrieval Processes

In corpus graph retrieval, retrieval outcomes are heavily influenced by the textual information associated with nodes. For instance, given  $q$  in Figure 1 (a) requesting an explanation of components for *Agentic RAG*, successfully retrieving node  $n_4$  requires recognizing that *Agentic RAG employs multi-step prompting strategies such as ReAct*. Crucially, this insight is derived from the textual content  $c_3$  of the intermediate node  $n_3$ , which is encountered along the retrieval path, rather than solely from the target node's content  $c_4$  or its vector representation  $\mathbf{V}_4$ .

We formalize this capability as *insightful retrieval*, which consists of two sub-processes inspired by complex iterative RAG methods [27, 30, 37, 39]:

- **(P1) Understanding:** The retriever analyzes the textual content of each visited node in the context of the query  $q$ .
- **(P2) Deciding:** Based on the understanding of  $c_i$ , the retriever determines which nodes should be traversed next.

## 3 Methodologies

### 3.1 Taxonomy for Graph Retrieval Operators

In a corpus graph  $\mathcal{G} = (\mathcal{N}, \mathcal{E})$ , a *retrieval operator*  $O$  is defined as a composite function  $\mathcal{P} \circ \mathcal{R}$ , where a **ranking function**  $\mathcal{R}$  scores nodes and a **pruning function**  $\mathcal{P}$  selects the final subset  $\mathcal{N}_{\text{ret}}$ . We classify them into three categories based on input sources and scoring mechanisms: Vector Search ( $O_{\text{vs}}$ ), Graph Search ( $O_{\text{gs}}$ ), and Model-based Search ( $O_{\text{m}}$ ). We detail definitions below.

**3.1.1 Vector Search Operator.** The **Vector Search Operator** ( $O_{\text{vs}}$ ) takes a query vector  $\mathbf{v}_q$  and the set of all nodes  $\mathcal{N}$  (associated with pre-indexed vectors  $\mathbf{V}$ ) as inputs. It employs a ranking function  $\mathcal{R}_{\text{VS}}$  to compute vector similarity, followed by a pruning function  $\mathcal{P}_{\text{VS}}$  that identifies the top- $k$  nodes. Formally,  $O_{\text{vs}}$  is defined as follows:

**Definition 2** (Vector Search,  $O_{\text{vs}}$ ). The Vector Search operator retrieves a node set  $\mathcal{N}_{\text{VS}}$  by

$$\begin{aligned}\mathcal{N}_{\text{VS}} &= O_{\text{vs}}(\mathbf{v}_q, \mathcal{N}, k) = \mathcal{P}_{\text{VS}}(\{\mathcal{R}_{\text{VS}}(\mathbf{v}_q, n) \mid n \in \mathcal{N}\}, k) \\ &= \arg \operatorname{topk} \sim(\mathbf{v}_q, \mathbf{v}_n)_{n \in \mathcal{N}}\end{aligned}$$

where  $\mathbf{v}_n$  denotes the vector representation of node  $n$ , and  $\sim(\cdot, \cdot)$  denotes a vector similarity metric.

**Example 1** (Dense Vector Search). In dense retrieval, the node vectors lie in a continuous latent manifold  $\mathbb{R}^d$ . The similarity is typically defined as the cosine similarity:

$$\sim(\mathbf{v}_q, \mathbf{v}_n) = \frac{\mathbf{v}_q^\top \mathbf{v}_n}{|\mathbf{v}_q| \cdot |\mathbf{v}_n|}$$

**3.1.2 Graph Search Operator.** The **Graph Search Operator** ( $O_{\text{gs}}$ ) takes a set of seed nodes  $\mathcal{N}_{\text{seed}} \subset \mathcal{N}$ , seed node features  $\mathbf{H}_{\text{seed}}$ , and the edge set  $\mathcal{E}$  as inputs. It employs a ranking function  $\mathcal{R}_{\text{GS}}$  to calculate topological scores  $\mathbf{H}^{(L)}$  via  $L$ -step signal propagation on  $\mathcal{E}$ , generalizing Graph Neural Networks (GNNs) message-passing. Unlike  $O_{\text{vs}}$ , the dependency of  $O_{\text{gs}}$  on  $\mathcal{N}_{\text{seed}}$  and  $\mathbf{H}_{\text{seed}}$  is crucial for (P2), as insightful retrieval necessitates outcomes that adapt to intermediate results.

**Definition 3** (Graph Search,  $O_{\text{gs}}$ ). The Graph Search operator retrieves a node set  $\mathcal{N}_{\text{GS}}$  by

$$\begin{aligned}\mathcal{N}_{\text{GS}} &= O_{\text{gs}}(\mathcal{N}_{\text{seed}}, \mathbf{H}_{\text{seed}}, \mathcal{E}) = \mathcal{P}_{\text{GS}}(\mathcal{R}_{\text{GS}}(\mathcal{N}_{\text{seed}}, \mathbf{H}_{\text{seed}}, \mathcal{E})) \\ &= \mathcal{P}_{\text{GS}}\left(\mathbf{H}^{(L)}\right)\end{aligned}$$

Here,  $\mathbf{H}^{(L)}$  denotes the node scores in  $\mathcal{N}$  after  $L$  steps. With  $\mathbf{H}^{(0)} = \mathbf{H}_{\text{seed}}$  initialized by the preceding retrieval, the  $l$ -th update rule is:

$$\mathbf{H}^{(l)} = f_{\text{prop}}^{(l)}\left(\mathcal{N}_{\text{seed}}, \mathbf{H}^{(l-1)}, \mathcal{E}\right)$$

**Example 2** (PageRank Retrieval). In PageRank-based retrieval [17, 25],  $\mathcal{R}_{\text{GS}}$  performs iterative propagation using the update function  $f_{\text{prop}}^{(l)}$  until  $\mathbf{H}^{(L)}$  converges, where  $f_{\text{prop}}^{(l)}$  is defined as:

$$\mathbf{H}^{(l)} = f_{\text{prop}}^{(l)}(\mathcal{N}_{\text{seed}}, \mathbf{H}^{(l-1)}, \mathcal{E}) = (1 - \alpha)\mathbf{M}\mathbf{H}^{(l-1)} + \alpha\mathbf{H}^{(0)}$$

where  $\alpha$  denotes the restart probability and  $\mathbf{M}$  is the column-normalized transition matrix derived from  $\mathcal{E}$ . Here,  $\mathbf{H}^{(0)}$  serves as the personalized restart distribution. The pruning function  $\mathcal{P}_{\text{GS}}$  selects the top- $k$  nodes with the highest scores as follows:

$$\mathcal{P}_{\text{GS}}(\mathbf{H}^{(L)}) = \arg \operatorname{topk} [\mathbf{H}^{(L)}]_n$$

**3.1.3 Model-based Search.** Third, the **Model-based Search** ( $O_{\text{m}}$ ) operator takes a textual query  $q$  and a set of seed nodes  $\mathcal{N}_{\text{seed}} \subseteq \mathcal{N}$  as inputs. In its ranking function  $\mathcal{R}_{\text{M}}$ , it utilizes a computationally intensive model  $P_{\phi}$  (e.g., a language model) to process the raw textual content of nodes and assess their relevance. Unlike  $O_{\text{vs}}$ ,  $O_{\text{m}}$  performs early interaction retrieval. Due to the high computational cost for this interaction, the operator is typically restricted to a small subset  $\mathcal{N}_{\text{seed}} \subset \mathcal{N}$ . Formally,  $O_{\text{m}}$  is defined as follows:

**Definition 4** (Model-based Search,  $O_{\text{m}}$ ). The Model-based Search operator selects a node set  $\mathcal{N}_{\text{M}}$  from  $\mathcal{N}_{\text{seed}} \subset \mathcal{N}$  by

$$\begin{aligned}\mathcal{N}_{\text{M}} &= O_{\text{m}}(q, \mathcal{N}_{\text{seed}}, k) = \mathcal{P}_{\text{M}}(\{\mathcal{R}_{\text{M}}(q, n) \mid n \in \mathcal{N}_{\text{seed}}\}, k) \\ &= \arg \operatorname{topk} P_{\phi}(q, n)_{n \in \mathcal{N}_{\text{seed}}}\end{aligned}$$

**Example 3** (Retrieve-then-Rerank Pipeline). Consider a standard pipeline employing a Bi-encoder (e.g., Contriever) for retrieval and a Cross-encoder (e.g., BERT) for reranking. While the overall process is neither  $O_{\text{vs}}$  nor  $O_{\text{m}}$ , we can divide the pipeline into two subprocesses:

- (1) *Candidate Retrieval:* The Bi-encoder retrieves the top-100 candidates ( $\mathcal{N}_{\text{cand}}$ ) based on cosine vector similarity with query vector  $\mathbf{v}_q = \text{Contriever}(q)$ . This instantiates  $O_{\text{vs}}$ :

$$\mathcal{N}_{\text{cand}} = \arg \operatorname{top100} \frac{\mathbf{v}_q^\top \mathbf{v}_n}{|\mathbf{v}_q| \cdot |\mathbf{v}_n|} = O_{\text{vs}}(\mathbf{v}_q, \mathcal{N}, 100)$$

- (2) *Reranking:* The Cross-encoder scores  $\mathcal{N}_{\text{cand}}$  given the query  $q$  to select the final top-10 nodes. This instantiates  $O_{\text{m}}$ :

$$\mathcal{N}_{\text{final}} = \arg \operatorname{topk}_{n \in \mathcal{N}_{\text{seed}}} \text{MLP}(\text{BERT}(q \oplus n)) = O_{\text{m}}(q, \mathcal{N}_{\text{cand}}, 10)$$

**3.1.4 Fusion Operators** ( $O_{\text{gm}}$ ,  $O_{\text{vgs}}$ ). To bridge the modality gaps in basic operators, where  $O_{\text{vs}}$  ignores topology and  $O_{\text{gs}}/O_{\text{m}}$  overlook semantics or neighbors, we propose two **fusion operators** that leverage both semantic and topological inputs to expand the search space.

First, to overcome the *topological blindness* of  $O_{\text{m}}$ , we define **Graph Model-based Search** ( $O_{\text{gm}}$ ), which integrates graph structure  $\mathcal{E}$  into relevance scoring.

**Definition 5** (Graph Model-based Search,  $O_{\text{gm}}$ ).  $O_{\text{gm}}$  selects nodes from  $\mathcal{N}_{\text{seed}} \subset \mathcal{N}$  by incorporating topological context  $\mathcal{E}$ :

$$\mathcal{N}_{\text{GM}} = O_{\text{gm}}(q, \mathcal{N}_{\text{seed}}, \mathcal{E}, k) = \mathcal{P}_{\text{GM}}(\mathcal{R}_{\text{GM}}(q, \mathcal{N}_{\text{seed}}, \mathcal{E}), k)$$

Second, to address the *semantic blindness* of  $O_{\text{gs}}$ , we introduce **Vector-Graph Search** ( $O_{\text{vgs}}$ ). It utilizes both the query vector  $\mathbf{v}_q$  and graph structure  $\mathcal{E}$  to identify semantically relevant yet structurally accessible nodes.

**Definition 6** (Vector-Graph Search,  $O_{\text{vgs}}$ ).  $O_{\text{vgs}}$  retrieves nodes using both vector representations  $\mathcal{V}$  and graph topology  $\mathcal{E}$ :

$$\mathcal{N}_{\text{VGS}} = O_{\text{vgs}}(\mathbf{v}_q, \mathcal{V}, \mathcal{N}_{\text{seed}}, \mathcal{E})$$

## 3.2 FastInsight Algorithm

The **FastInsight** algorithm takes the following inputs: a query  $q$ , a corpus graph  $\mathcal{G} = (\mathcal{N}, \mathcal{E})$ , a query vector  $\mathbf{v}_q$ , a set of node vectors  $\mathcal{V}$ , and a set of *hyperparameters* ( $\text{BATCH}$ ,  $\alpha$ ,  $\beta$ , and  $b_{\max}$ ). The output is a list of retrieved nodes,  $\mathcal{N}_{\text{ret}}$ .

The execution flow of FastInsight is outlined in Algorithm 1. In this algorithm, each colored box represents a retrieval operator:  $O_{\text{vs}}$  (Vector Search),  $O_{\text{gm}}$  (Graph Model-based Search), and

$O_{\text{vgs}}$  (Vector-Graph Search). The process comprises two primary phases: the **initial setup step** and the **iterative retrieval step**. We explain these steps in detail below.

---

### Algorithm 1 The FastInsight algorithm

---

**Input:** Query  $q$ , Graph  $\mathcal{G} = (\mathcal{N}, \mathcal{E})$ , Node vectors  $\mathcal{V} = \{\text{Enc}_N(n_i) \mid n_i \in \mathcal{N}\}$ , Query vector  $\mathbf{v}_q = \text{Enc}_Q(q)$ , Batch size  $\text{BATCH}$ , Smoothing factor  $\alpha$ , Score ratio  $\beta$ , Budget  $b_{\max}$

**Output:**  $\mathcal{N}_{\text{ret}}$  (List of retrieved nodes)

- ```

1:  $\mathcal{N}_{\text{ret}} \leftarrow \arg \operatorname{topk}_{n \in \mathcal{N}} \text{sim}(\mathbf{v}_q, \mathcal{V}_n)$  1. Initial  $O_{\text{vs}}$ 
2:  $\mathcal{N}_{\text{ret}} \leftarrow \text{GRanker}(q, \mathcal{N}_{\text{ret}}, \mathcal{E}, \alpha)$  2.  $O_{\text{gm}}$  using  $\text{GRanker}$ 
3: while  $|\mathcal{N}_{\text{ret}}| < b_{\max}$  do 3. Expansion Loop with  $O_{\text{vgs}}$ 
4:    $\mathcal{N}_{\text{add}} \leftarrow \text{STeX}(\mathbf{v}_q, \mathcal{V}, \mathcal{E}, \mathcal{N}_{\text{ret}}, \beta)$   $O_{\text{vgs}}$  using  $\text{STeX}$ 
5:    $k_{\text{remain}} \leftarrow \min(|\mathcal{N}_{\text{ret}}| + \text{BATCH}, b_{\max}) - |\mathcal{N}_{\text{ret}}|$ 
6:    $\mathcal{N}_{\text{ret}} \leftarrow \mathcal{N}_{\text{ret}} \cup \mathcal{N}_{\text{add}}[:k_{\text{remain}}]$  Apply hard budget cap
7:    $\mathcal{N}_{\text{ret}} \leftarrow \text{GRanker}(q, \mathcal{N}_{\text{ret}}, \mathcal{E}, \alpha)$   $O_{\text{gm}}$  using  $\text{GRanker}$ 
8: end while
9: return  $\mathcal{N}_{\text{ret}}$ 

```
- 

*Initial setup step* (Lines 1–2). In this step, the retriever establishes the starting nodes for the subsequent iterative process.

- **(L1)** First, a dot product-based vector search is performed on the node vectors  $\mathcal{V}$  to retrieve a top-BATCH list of candidates,  $\mathcal{N}_{\text{ret}}$ , sorted by their dot product scores.
- **(L2)** The GRanker method is applied to assign initial relevance scores to these nodes.

*Iterative retrieval step (Lines 3–9).* In this step, the retriever iteratively expands the selected node list  $\mathcal{N}_{\text{ret}}$  until its size reaches the maximal budget  $b_{\max}$ . By employing this iterative process, FastInsight enhances the quality of the input nodes  $\mathcal{N}_{\text{ret}}$  fed into GRanker, allowing us to produce better retrieval outcomes while minimizing the usage of GRanker (i.e., minimize computational cost).

- **(L4)** In each iteration, the STeX algorithm ( $O_{\text{vgs}}$  operator) identifies potential new nodes ( $\mathcal{N}_{\text{add}}$ ) based on the current  $\mathcal{N}_{\text{ret}}$ .
- **(L5–L6)** The retriever then incorporates up to BATCH new nodes into  $\mathcal{N}_{\text{ret}}$  (strictly adhering to the budget cap  $b_{\max}$ ).
- **(L7)** For the next iteration, the retriever re-applies GRanker to update the rankings of the retrieved nodes  $\mathcal{N}_{\text{ret}}$ .

The hyperparameters control the algorithm's behavior as follows: BATCH denotes the number of nodes added to  $\mathcal{N}_{\text{ret}}$  during a single iteration;  $\alpha$  represents the smoothing factor for GRanker (detailed in Section 3.3);  $\beta$  represents the score ratio for STeX (in Section 3.4) and  $b_{\max}$  defines the maximum node budget, serving as the stopping criterion for the iterative loop.

### 3.3 GRanker for Graph Model-based Search

As the first effective implementation of the  $O_{\text{gm}}$  operator defined in Definition 5, we propose the **Graph-based Reranker (GRanker)**. To address Challenge 1, we interpret the initial cross-encoder embeddings  $\mathbf{H}$  as noisy signals, as they are generated in a topology-blind manner. Consequently, GRanker frames the task as a *graph signal denoising problem*, aiming to smooth  $\mathbf{H}$  by leveraging  $\mathcal{E}$ . This corresponds to minimizing the Laplacian-regularized objective:

$$\mathcal{L}(\mathbf{H}') = \frac{1}{2} \|\mathbf{H}' - \mathbf{H}\|_F^2 + \frac{\lambda}{2} \text{Tr}(\mathbf{H}'^\top \mathbf{L}_{rw} \mathbf{H}')$$

where  $\mathbf{L}_{rw} = \mathbf{I} - \mathbf{P}$  is the random-walk Laplacian. Instead of the computationally expensive closed-form solution, we employ a *first-order approximation* via a single gradient descent step. This yields our efficient update rule:

$$\mathbf{H}' \leftarrow \mathbf{H} - \eta \nabla \mathcal{L}(\mathbf{H}) = (1 - \alpha)\mathbf{H} + \alpha(\mathbf{P}\mathbf{H}')$$

where  $\alpha = \eta\lambda$ . Algorithm 2 details this process, where Lines 2–7 introduce our refinements to the standard reranking workflow. The detailed procedure of these steps is as follows:

- **(L2–L5) Propagation Matrix Construction:** GRanker constructs a normalized propagation matrix  $\mathbf{P}$  from the subgraph's adjacency ( $\mathbf{A}$ ) and degree ( $\mathbf{D}$ ) matrices. By using the reciprocal of node degrees,  $\mathbf{P}$  balances the influence of high-degree nodes during aggregation.
- **(L6) Latent Graph Fusion:** The initial latent vectors  $\mathbf{H}$  are smoothed with neighbor-aggregated context ( $\mathbf{P} \cdot \mathbf{H}$ ) via graph convolution. The factor  $\alpha$  controls the trade-off between intrinsic semantics and structural support, resulting in fused representations  $\mathbf{H}'$ .

---

### Algorithm 2 Our GRanker method for $O_{\text{gm}}$

**Input:** Query  $q$ , Retrieved  $\mathcal{N}_{\text{ret}}$ , Edges  $\mathcal{E}$ , Smoothing factor  $\alpha$   
**Output:** Reranked list of nodes  $\mathcal{N}_{\text{ret}}$   
**Inner function:** Encoder( $\cdot$ ) for latent vector extraction, MLP( $\cdot$ ) for scoring,  $\deg_{\mathcal{E}}(\cdot)$  for node degree calculation

```

1:  $\mathbf{H} \leftarrow [\text{Encoder}(q, n_i)]_{n_i \in \mathcal{N}_{\text{ret}}}$            ▷ Extract Latent Vectors
2:  $\mathbf{A} \in \{0, 1\}^{|\mathcal{N}_{\text{ret}}| \times |\mathcal{N}_{\text{ret}}|}$  where  $A_{ij} = \mathbb{I}((n_i, n_j) \in \mathcal{E})$ 
3:  $\mathbf{D} \in \mathbb{R}^{|\mathcal{N}_{\text{ret}}| \times |\mathcal{N}_{\text{ret}}|}$  where  $D_{ii} = \deg_{\mathcal{E}}(n_i)$ 
4:  $\mathbf{W} \leftarrow \mathbf{A} \cdot \mathbf{D}^{-1}$            ▷ Weighting by reciprocal of degrees
5:  $\mathbf{P} \leftarrow \text{diag}(\mathbf{W} \cdot \mathbf{1})^{-1} \cdot \mathbf{W}$       ▷ Normalized Propagation Matrix
6:  $\mathbf{H}' \leftarrow (1 - \alpha)\mathbf{H} + \alpha(\mathbf{P}\mathbf{H})$           ▷ Latent Graph Fusion
7:  $\mathbf{S} \leftarrow \text{MLP}(\mathbf{H}')$                       ▷ Scoring via Classifier Head
8:  $\mathcal{N}_{\text{ret}} \leftarrow \text{argsort}(\mathcal{N}_{\text{ret}}, \text{score}=\mathbf{S})$ 
9: return  $\mathcal{N}_{\text{ret}}$ 

```

---

- **(L7) Semantic Scoring:** The final relevance scores  $\mathbf{S}$  are computed by passing  $\mathbf{H}'$  through the MLP head, ensuring the ranking incorporates both semantic relevance and topological evidence.

### 3.4 STeX for Vector-Graph Search

We propose **Semantic-Topological eXpansion (STeX)**, the first fast and effective implementation of the  $O_{\text{vgs}}$  that identifies candidates by leveraging both topological structure and semantic representations, unlike conventional topology-only methods. As detailed in Algorithm 3, the procedure ranks candidates in  $\mathcal{N}_{\text{STeX}}$  using a composite score—a  $\beta$ -weighted sum of structural importance ( $I_{\text{Struct}}$ ) and semantic similarity ( $I_{\text{Sim}}$ ):

- $I_{\text{Struct}}$  (**Lines 3–12**): This score integrates *rank proximity* and *bridging capability*. It captures proximity to high-ranking context by favoring candidates connected to the highest-ranked nodes ( $r_{best}$ ) in  $\mathcal{N}_{\text{ret}}$ . Additionally, it incorporates a bridging factor  $|A(n)|$  that rewards nodes acting as information brokers across the graph structure, inspired by *Structural Hole Theory* [6, 14].
- $I_{\text{Sim}}$  (**Line 13**): This is the dot product similarity between the query  $v_q$  and the candidate vector  $\mathcal{V}_n$ . This ensures that semantically relevant nodes are preserved even if they are topologically distant.

## 4 Experiments

We conduct two types of experiments: (1) *a retrieval experiment*, which aims to retrieve  $\mathcal{N}_{\text{ret}}$  for a given query  $q$ , and (2) *a RAG experiment*, which focuses on generating responses based on  $\mathcal{N}_{\text{ret}}$ . Unless otherwise specified, we use OpenAI's text-embedding-3-small as the embedding model, OpenAI's gpt-5-mini as the generative LLM, and bge-reranker-v2-m3 as the reranker. For RQ2 (Efficiency), we use two server configurations: (a) eight NVIDIA 24GB TITAN GPUs and (b) six NVIDIA 80GB A100 GPUs. All other experiments, except those for efficiency evaluation, are conducted via configuration (a).

### 4.1 Retrieval and RAG Baselines

**4.1.1 Retrieval Baselines.** We evaluate retrieval performance using five document retrieval baselines and four graph retrieval baselines. While many Graph RAG methods designed for KGs are incompatible with corpus graphs, we include HippoRAG 2 [17] by adapting it to

**Algorithm 3** Our STeX method for  $O_{\text{vgs}}$ 


---

**Input:** Query vector  $v_q$ , Node vectors  $\mathcal{V}$ , Edges  $\mathcal{E}$ , Retrieved  $\mathcal{N}_{\text{ret}}$ , Score ratio  $\beta$ .

**Inner function:**  $\text{rankCheck}(n)$  checks the rank of  $n$ ,  $\deg_{\mathcal{E}}(\cdot)$

**Output:** Set of nodes to add  $\mathcal{N}_{\text{add}}$

```

1:  $\mathcal{N}_{\text{STeX}} \leftarrow \{n_j \mid \exists_{n_i \in \mathcal{N}_{\text{ret}}} (n_i, n_j) \in \mathcal{E}\} \setminus \mathcal{N}_{\text{ret}}, R_{\max} \leftarrow |\mathcal{N}_{\text{ret}}|$ 
2: for  $n \in \mathcal{N}_{\text{STeX}}$  do
3:    $I_{\text{Struct}} \leftarrow 0$ 
4:    $A(n) \leftarrow \{v \in \mathcal{N}_{\text{ret}} \mid (n, v) \in \mathcal{E}\}$  ▷ Adjacent retrieved nodes
5:   if  $R_{\max} > 1$  then
6:      $r_{\text{best}} \leftarrow \min\{\text{rankCheck}(v, \mathcal{N}_{\text{ret}}) \mid v \in A(n)\}$ 
7:      $I_{\text{Struct}} \leftarrow 1 - \frac{r_{\text{best}} - 1}{R_{\max} - 1}$ 
8:   end if
9:    $C_{\max} \leftarrow \min(\deg_{\mathcal{E}}(n), R_{\max})$ 
10:  if  $C_{\max} > 1$  then
11:     $I_{\text{Struct}} \leftarrow I_{\text{Struct}} + \frac{|A(n)| - 1}{C_{\max} - 1}$  ▷ 1. Structural score ( $I_{\text{Struct}}$ )
12:  end if
13:   $I_{\text{Sim}} \leftarrow v_q \cdot \mathcal{V}_n$  ▷ 2. Similarity score ( $I_{\text{Sim}}$ )
14:   $S_n \leftarrow I_{\text{Sim}} + \beta \cdot (I_{\text{Struct}})$ 
15: end for
16:  $\mathcal{N}_{\text{add}} \leftarrow \text{argsort}(\mathcal{N}_{\text{STeX}}, \text{score} = S)$ 
17: return  $\mathcal{N}_{\text{add}}$ 

```

---

the corpus graph setting. Other methods that cannot be applied to corpus graphs are excluded.

Five document retrieval baselines rely on vector search ( $O_{\text{vs}}$ ) or model-based reranking ( $O_{\text{m}}$ ). We include (1) **Vector Search** ( $O_{\text{vs}}$ ): retrieves nodes based on dot product similarity; (2-3) **SPLADE** [11] ( $O_{\text{vs}}$ ) and **Contriever** [22] ( $O_{\text{vs}}$ ): representative sparse and dense retrieval methods, respectively; (4) **HyDE** [12] ( $O_{\text{vs}}$ ): performs retrieval using generated hypothetical documents; and (5) **Retrieve-then-Rerank (Re2)** ( $O_{\text{vs}}, O_{\text{m}}$ ): reranks the top-100 candidates retrieved by Vector Search.

Four graph retrieval baselines and FastInsight incorporate graph topology via the graph search operator ( $O_{\text{gs}}$ ). We include (1) **GAR** [31] ( $O_{\text{vs}}, O_{\text{gs}}, O_{\text{m}}$ ): dynamically interleaves vector and graph search with iterative reranking ( $b_{\max} = 100, \text{BATCH} = 10$ ); (2-3) **LightRAG/PathRAG** [7, 15] ( $O_{\text{vs}}, O_{\text{gs}}$ ): refine queries using keywords generated by gpt-4o-mini, prior to executing  $O_{\text{vs}}$  and  $O_{\text{gs}}$ ; and (4) **HippoRAG 2** ( $O_{\text{vs}}, O_{\text{gs}}$ ): a KG-based method that we adapted to perform retrieval on corpus graph topology. Finally, our **FastInsight** ( $O_{\text{vs}}, O_{\text{vgs}}, O_{\text{gm}}$ ): utilizes frozen [CLS] features extracted from the reranker (pre-MLP) to initialize  $H$ , leverages the last two layers of its classification head as  $MLP(\cdot)$ , and sets  $b_{\max} = 100, \text{BATCH} = 10, \alpha = 0.2$ , and  $\beta = 1$ .

**4.1.2 RAG Baselines.** We generate responses by feeding the nodes retrieved by each retriever in the retrieval experiment into OpenAI's GPT-5-nano model. Consequently, the RAG experiment includes a total of 10 methods, nine baselines and FastInsight.

## 4.2 Datasets

**4.2.1 The ACL-OCL dataset.** ACL OCL [35] is a text corpus derived from ACL Anthology, comprising approximately 80k academic papers with references and full texts. To evaluate baseline models on reference networks, we transform this corpus into the *ACL-OCL dataset*, which will be publicly released, specifically designed to

assess both retrieval and generation performance. Unlike existing datasets, ACL-OCL emphasizes scenarios where retrieving the correct answer requires understanding the semantic and structural context of intermediate nodes. We construct the dataset through two stages: *reference network construction* and *synthetic query generation*.

**Reference Network Construction.** Each paper is divided into chunks of 4,096 characters, which constitute the node set  $\mathcal{N}$ . To construct the edge set  $\mathcal{E}$  while mitigating spurious edges caused by paper-level metadata, we employ a reference detection model that identifies explicit citations within each chunk  $n$ . For each detected citation, we create an edge  $(n, n_i)$  linking the chunk to the cited paper's corresponding node(s). This model is implemented using GPT-5-nano via in-context learning. Detailed statistics are in Table 2.

**Synthetic Query Generation.** We generate synthetic query-gold node pairs by selecting connected node pairs and prompting an LLM to formulate questions that require information from both. This design intentionally targets the evaluation of **Insightful Retrieval**, as answering these queries necessitates interpreting intermediate node contents to bridge the semantic gap between the query and the target answer. In total, we generated 753 queries, as illustrated in Figure 2.

### Query

What visualization approach and export formats does the web-based annotation tool mentioned in **LIDA** use to render complex, overlapping text annotations and produce figures for publications?

### Related Nodes (Gold Nodes)

#### LIDA node chunk #2:

**BRAT (Stenetorp et al., 2012)** and Doccanno 3 are web-based annotation tools [...]. **LIDA** aims to fill these gaps by providing [...]

#### BRAT node chunk #1:

BRAT is based on our previously released opensource STAV text annotation visualiser [...]. Both tools share a **vector graphics-based visualisation** component [...] **BRAT integrates PDF and EPS image format** export [...]

**Figure 2: Example of synthetic query generation.** Red indicates textual reference to the BRAT node, while blue indicates the answer.

**4.2.2 Datasets for Experiments.** To evaluate retrieval performance, we use a total of five datasets spanning two types of corpus graphs: ACL-OCL and LACD [1] for reference networks, and BSARD-G, SciFact-G, and NFCorpus-G for text-rich knowledge graphs. As there are currently no established IR benchmarks specifically designed for text-rich knowledge graphs, we adapt three widely used IR benchmarks—BSARD [29], SciFact [40], and NFCorpus [4]—into graph-based formats following the graph construction procedure used in LightRAG. For ground-truth relevance, we define all nodes constructed from the original gold documents as gold nodes.

For the RAG experiment, we use ACL-OCL for reference networks and two datasets from *UltraDomain* [33] for text-rich knowledge graphs. We excluded LACD, SciFact and NFCorpus from the RAG evaluation, as they are not formatted as QA datasets. Detailed statistics for all datasets are summarized in Table 2.

**Table 2: Dataset statistics for retrieval and RAG experiments.**  
**UD:** UltraDomain datasets; Gray shading: reference networks.

| Datasets       | Purpose     | Domain      | N       | E         | Q     |
|----------------|-------------|-------------|---------|-----------|-------|
| ACL-OCL        | Ret. & Gen. | CS          | 402,742 | 5,840,449 | 753   |
| LACD           | Retrieval   | Legal       | 192,974 | 339,666   | 89    |
| BSARD-G        | Ret. & Gen. | Legal       | 56,728  | 92,672    | 222   |
| SciFact-G      | Retrieval   | Science     | 36,438  | 43,557    | 1,109 |
| NFCorpus-G     | Retrieval   | Medical     | 23,468  | 27,805    | 3,237 |
| UD-agriculture | Generation  | Agriculture | 46,561  | 82,088    | 100   |
| UD-mix         | Generation  | Mix         | 11,812  | 10,384    | 130   |

### 4.3 Metrics

**4.3.1 Conventional Metrics.** To evaluate retrieval performance, we use Capped Recall score ( $R@k$ ) and Normalized Discounted Cumulative Gain (nDCG), both evaluated at **top-10**. Capped Recall [38] normalizes the maximum achievable recall to 1 when selecting the top- $k$  nodes. For generation evaluation, we adopt a pairwise LLM-as-a-Judge approach, following the evaluation protocol and prompts used in LightRAG [15], where a generative LLM serves as the evaluator.

**4.3.2 Topological Recall.** To quantify *insightful retrieval*, we introduce a new metric named **Topological Recall (TR)**, defined over the range  $[0, 1]$ . Unlike conventional Recall, TR captures the graph-theoretic proximity between retrieved nodes  $\mathcal{N}_{\text{ret}}$  to oracle nodes  $\mathcal{N}_{\text{oracle}}$  by modeling shortest path *uncertainty*.

**Definition 7** (Topological Recall). For given  $\mathcal{E}, \mathcal{N}_{\text{ret}}, \mathcal{N}_{\text{oracle}}$ :

$$TR(\mathcal{E}, \mathcal{N}_{\text{ret}}, \mathcal{N}_{\text{oracle}}) = \text{avg}_{n_i \in \mathcal{N}_{\text{oracle}}} \left( \frac{1}{1 + u(\mathcal{E}, \mathcal{N}_{\text{ret}}, n_i)} \right)$$

where the uncertainty function  $u$  is defined as the accumulated log-degree along the shortest path:

$$u(\mathcal{E}, \mathcal{N}_{\text{ret}}, n_i) = \min_{n_j \in \mathcal{N}_{\text{ret}}} \sum_{n_k \in SP(\mathcal{E}, n_j, n_i), n_k \neq n_i} \ln(1 + \deg_{\mathcal{E}}(n_k))$$

Here,  $SP(\mathcal{E}, n_j, n_i)$  denotes the set of nodes on the shortest path from the seed node  $n_j$  to the oracle node  $n_i$ .

Importantly, TR extends conventional Recall by assigning partial credit to oracle nodes that are not directly retrieved but are close in the graph. To formalize this relationship and provide a theoretical foundation for its application in future research, we present the following decomposition as a corollary along with its proof.

**Corollary 1** (Decomposition). For given  $\mathcal{E}, \mathcal{N}_{\text{ret}}, \mathcal{N}_{\text{oracle}}$ , TR and Recall for  $\mathcal{N}_{\text{ret}}$  have the following relationship:

$$TR = Recall + \frac{|\mathcal{N}_{\text{oracle}} \setminus \mathcal{N}_{\text{ret}}|}{|\mathcal{N}_{\text{oracle}}|} \cdot TR(\mathcal{E}, \mathcal{N}_{\text{ret}}, \mathcal{N}_{\text{oracle}} \setminus \mathcal{N}_{\text{ret}})$$

**PROOF.** Let  $\mathcal{N}_{\text{found}} = \mathcal{N}_{\text{oracle}} \cap \mathcal{N}_{\text{ret}}$  and  $\mathcal{N}_{\text{miss}} = \mathcal{N}_{\text{oracle}} \setminus \mathcal{N}_{\text{ret}}$ . Note that for any  $n_i \in \mathcal{N}_{\text{found}}$ , the uncertainty  $u(\mathcal{E}, \mathcal{N}_{\text{ret}}, n_i) = 0$ . By decomposing the summation in the definition of TR:

$$\begin{aligned} TR &= \frac{1}{|\mathcal{N}_{\text{oracle}}|} \left( \sum_{n_i \in \mathcal{N}_{\text{found}}} 1 + \sum_{n_i \in \mathcal{N}_{\text{miss}}} \frac{1}{1 + u(\mathcal{E}, \mathcal{N}_{\text{ret}}, n_i)} \right) \\ &= \underbrace{\frac{|\mathcal{N}_{\text{found}}|}{|\mathcal{N}_{\text{oracle}}|}}_{\text{Recall}} + \underbrace{\frac{|\mathcal{N}_{\text{miss}}|}{|\mathcal{N}_{\text{oracle}}|} \left( \frac{1}{|\mathcal{N}_{\text{miss}}|} \sum_{n_i \in \mathcal{N}_{\text{miss}}} \frac{1}{1 + u(\mathcal{E}, \mathcal{N}_{\text{ret}}, n_i)} \right)}_{TR(\mathcal{E}, \mathcal{N}_{\text{ret}}, \mathcal{N}_{\text{miss}})} \quad \square \end{aligned}$$

Hereafter, we refer to  $\frac{|\mathcal{N}_{\text{oracle}} \setminus \mathcal{N}_{\text{ret}}|}{|\mathcal{N}_{\text{oracle}}|} \cdot TR(\mathcal{E}, \mathcal{N}_{\text{ret}}, \mathcal{N}_{\text{oracle}} \setminus \mathcal{N}_{\text{ret}})$  as *MissTR*, meaning the partial credit for missing oracle nodes. In Section 5.3, we analyze FastInsight's capability for insightful retrieval using TR and MissTR.

## 5 Result and Analysis

### 5.1 Effectiveness Analysis (RQ1)

**5.1.1 Retrieval Experiments.** Table 3 presents the performance of FastInsight and nine baselines for the retrieval pipeline across five graph retrieval datasets. Overall, our FastInsight method demonstrates robust and consistent performance improvements across all evaluated datasets. Compared to the strongest baseline in terms of overall average performance, **FastInsight achieves an improvement of 9.9% in R@10 and 9.1% in nDCG@10**.

Specifically, FastInsight significantly outperforms Re2, the strongest document retrieval baseline, by an average of **20.0% in R@10 and 17.7% in nDCG@10**. Furthermore, compared to GAR, which is the most competitive graph retrieval baseline, FastInsight yields substantial gains, particularly in reference networks. For instance, in the ACL-OCL dataset, our method surpasses GAR by a relative margin of **28.4% in R@10 and 30.5% in nDCG@10**, while the PathRAG method fails to run in time due to its complex flow algorithm. These results highlight the effectiveness of our approach in navigating complex graph structures.

**5.1.2 RAG Experiments.** Table 4 presents overall win rates comparing baselines and our method over four datasets. Here, FastInsight demonstrates superior performance in the RAG setting, consistently achieving **average win rates exceeding 55% against all baselines**. To investigate this improvement, we analyze the Pearson correlation between retrieval accuracy ( $R@10$ ) and generation quality (win rate) on the ACL-OCL and BSARD-G datasets, as they are the only ones that support both retrieval and generation tasks. As shown in Figure 3, we observe a significantly strong positive correlation with  $p < 0.05$ . It suggests that the retrieval enhancements from our method translate into more effective generation, indicating that employing FastInsight as a retriever strengthens the overall Graph RAG capability.

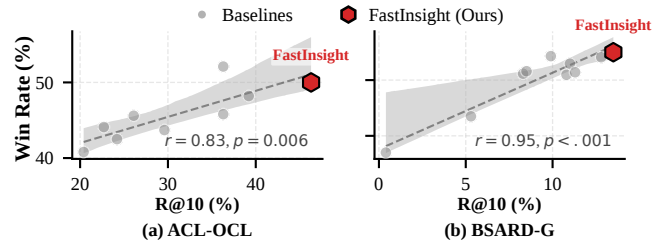


**Figure 3: Correlation between R@10 and Win Rate.** FastInsight is the self-reference baseline (50% win rate). Dashed lines and grey areas denote linear regression fits and 95% CIs.

### 5.2 Efficiency Analysis (RQ2)

**5.2.1 Query Processing Time Analysis.** To demonstrate time-efficiency, we compare the *Query Processing Time (QPT)* and  $R@10$  of FastInsight against baselines Re2 and GAR across TITAN and A100 GPUs. Figure 4 illustrates the QPT and  $R@10$  trade-off on ACL-OCL and

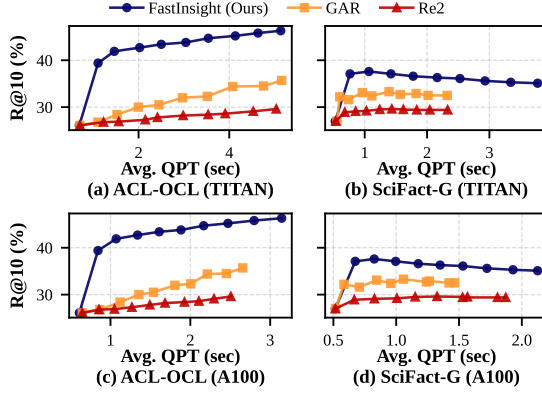
**Table 3: Retrieval results on five corpus graph datasets. All metrics are reported in percentage (%). The best results are highlighted in bold, and the second-best results are underlined. *Out-of-time* means that the method takes more than one hour per query.**

| Methods                   | Reference Networks |             |             |             | Text-rich Knowledge Graphs |             |             |             |             |             | Average     |             |
|---------------------------|--------------------|-------------|-------------|-------------|----------------------------|-------------|-------------|-------------|-------------|-------------|-------------|-------------|
|                           | ACL-OCL            |             | LACD        |             | BSARD-G                    |             | SciFact-G   |             | NFCorpus-G  |             | Overall     |             |
|                           | R@10               | nDCG@10     | R@10        | nDCG@10     | R@10                       | nDCG@10     | R@10        | nDCG@10     | R@10        | nDCG@10     | R@10        | nDCG@10     |
| <b>Document Retrieval</b> |                    |             |             |             |                            |             |             |             |             |             |             |             |
| Vector Search             | 26.1               | 19.6        | 38.1        | 26.4        | 8.3                        | 9.5         | 27.0        | 32.4        | 32.9        | 35.5        | 26.5        | 24.7        |
| SPLADE [11]               | 39.2               | <u>33.2</u> | 0.0         | 0.0         | 5.3                        | 5.8         | 27.2        | 32.5        | 33.8        | 36.1        | 21.1        | 21.5        |
| Contriever [22]           | 20.4               | 16.0        | 1.1         | 0.9         | 0.4                        | 0.3         | 27.7        | 32.5        | 35.2        | 37.7        | 17.0        | 17.5        |
| HyDE [12]                 | 22.7               | 17.1        | 39.2        | 26.3        | 9.9                        | 11.5        | 29.8        | 35.7        | <u>37.0</u> | <b>40.0</b> | 27.7        | 26.1        |
| Re2                       | 29.6               | 24.3        | 47.9        | 33.1        | 10.8                       | 12.2        | 29.4        | 34.7        | <u>34.6</u> | 37.1        | 30.5        | 28.3        |
| <b>Graph Retrieval</b>    |                    |             |             |             |                            |             |             |             |             |             |             |             |
| LightRAG [15]             | 24.2               | 15.7        | 19.3        | 12.0        | 11.0                       | 10.2        | 31.4        | 32.0        | 34.3        | 35.4        | 24.0        | 21.1        |
| PathRAG [7]               | <i>Out-of-time</i> | 0.0         | 0.0         | 11.3        | 11.7                       | 14.4        | 14.8        | 31.6        | 33.4        | 14.3        | 15.0        |             |
| HippoRAG 2 [17]           | 28.8               | 21.6        | 38.2        | 26.8        | 8.5                        | 9.8         | 27.0        | 32.4        | 32.9        | 35.5        | 27.1        | 25.2        |
| GAR [31]                  | 36.3               | 30.8        | 48.6        | <u>33.8</u> | <u>12.8</u>                | <u>13.8</u> | <u>32.5</u> | <u>37.1</u> | 36.4        | 38.6        | <u>33.3</u> | 30.8        |
| <b>FastInsight (Ours)</b> | <b>46.3</b>        | <b>40.2</b> | <b>50.3</b> | <u>35.0</u> | <u>13.7</u>                | <u>13.9</u> | <u>35.1</u> | <u>39.4</u> | <u>37.6</u> | <u>39.3</u> | <u>36.6</u> | <b>33.6</b> |

**Table 4: Overall Win Rates (%) of Baselines v.s. FastInsight across Four Datasets and Average.**

| Baselines     | ACL-OCL            |             | BSARD-G     |             | UltraDomain-agriculture |             | UltraDomain-mix |             | Average     |             |
|---------------|--------------------|-------------|-------------|-------------|-------------------------|-------------|-----------------|-------------|-------------|-------------|
|               | Baseline           | FastInsight | Baseline    | FastInsight | Baseline                | FastInsight | Baseline        | FastInsight | Baseline    | FastInsight |
| Vector Search | 45.6               | <b>53.3</b> | 42.3        | <b>57.2</b> | 43.0                    | <b>55.0</b> | 40.8            | <b>57.7</b> | 42.9        | <b>55.8</b> |
| SPLADE        | 48.2               | <b>51.7</b> | 27.0        | <b>72.5</b> | 43.0                    | <b>57.0</b> | 45.4            | <b>54.6</b> | 40.9        | <b>59.0</b> |
| Contriever    | 40.8               | <b>58.2</b> | 14.0        | <b>85.6</b> | 42.0                    | <b>56.0</b> | 46.2            | <b>53.1</b> | 35.8        | <b>63.2</b> |
| HyDE          | 44.1               | <b>55.4</b> | 48.6        | <b>51.4</b> | 44.0                    | <b>56.0</b> | 41.5            | <b>58.5</b> | 44.5        | <b>55.3</b> |
| Re2           | 43.7               | <b>55.1</b> | 41.9        | <b>57.7</b> | 3.0                     | <b>95.0</b> | 49.2            | <b>50.8</b> | 34.5        | <b>64.6</b> |
| LightRAG      | 42.5               | <b>57.1</b> | 45.9        | <b>53.6</b> | 39.0                    | <b>60.0</b> | 45.4            | <b>53.1</b> | 43.2        | <b>55.9</b> |
| PathRAG       | <i>Out-of-time</i> | 42.8        | <b>56.8</b> | 38.0        | <b>62.0</b>             | 23.1        | <b>76.2</b>     | 34.6        | <b>65.0</b> |             |
| HippoRAG 2    | 45.8               | <b>53.5</b> | 43.2        | <b>56.8</b> | 46.0                    | <b>53.0</b> | 35.4            | <b>63.1</b> | 42.6        | <b>56.6</b> |
| GAR-RAG       | <b>52.1</b>        | 47.1        | 48.2        | <b>51.8</b> | 38.0                    | <b>61.0</b> | 39.2            | <b>60.0</b> | 44.4        | <b>55.0</b> |

SciFact-G. Each data point represents a different number of  $O_m$  operators ( $b_{\max}$ ), from 10 to 100. As shown by the curves, FastInsight achieves a **Pareto improvement**, consistently delivering higher R@10 without compromising efficiency on both datasets.

**Figure 4: Scatter plots illustrating the trade-off between Average QPT and R@10 on (a,c) ACL-OCL, and (b,d) SciFact-G.**

**5.2.2 FastInsight versus Conventional Interleaving Retrieval.** To demonstrate FastInsight’s efficiency over computationally intensive interleaving retrieval, we compare it against IRCoT + Vector Search [39] on SciFact-G. To examine QPT fairly, we use a locally hosted Gemma 3 (12B) via Ollama in TITAN and A100 GPUs. IRCoT is configured with a 2-step process, retrieving 5 nodes per step.

As shown in Table 5, while IRCoT slightly improves Vector Search accuracy, it substantially increases latency due to iterative LLM inference. FastInsight effectively overcomes this bottleneck. Results confirm that our method reduces **query processing time**

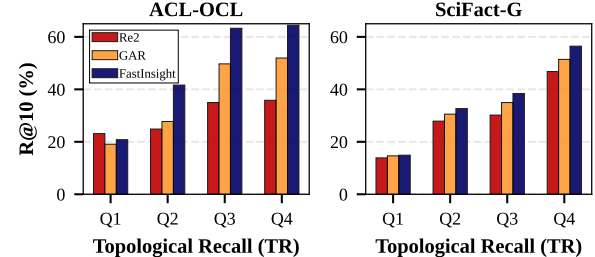
by 42–58% while improving R@10 by 11.7% compared to IRCoT, validating it as a time-efficient alternative.

**Table 5: Time efficiency on SciFact-G: FastInsight vs. IRCoT.**

| Method                    | R@10        | QPT (TITAN)              | QPT (A100)               |
|---------------------------|-------------|--------------------------|--------------------------|
| IRCoT + Vector Search     | 31.4        | 6.54 sec                 | 5.03 sec                 |
| <b>FastInsight (Ours)</b> | <b>35.1</b> | <b>3.77 sec (▼42.4%)</b> | <b>2.12 sec (▼57.9%)</b> |

### 5.3 Insightful Retrieval Analysis (RQ3)

**5.3.1 Topological Recall (TR) Analysis.** In this section, we analyze how well FastInsight performs *insightful retrieval* by leveraging the Topological Recall (TR) metric defined in Section 4.3.2. We validate whether TR effectively quantifies the topological proximity to oracle nodes and how our method exploits this proximity compared to baselines.

**Figure 5: Impact of Topological Recall (TR) on Retrieval Performance (R@10).**

**Impact of Topological Proximity.** We first investigate the relationship between TR and the standard Recall (R@10) to understand how topological proximity translates to retrieval performance. Figure

5 illustrates the distribution of R@10 across TR quartiles. As expected, all methods demonstrate improved Recall with increasing TR, confirming that higher TR implies closer proximity to oracle nodes and creates a topologically favorable state that facilitates the discovery of remaining oracle nodes. Critically, graph traversal methods (FastInsight and GAR) exhibit a steeper performance gain in the Q3-Q4 intervals compared to Vector Search-only baseline Re2. This indicates that graph-based methods successfully exploit the topological structure to retrieve oracle nodes Re2 fails to reach. Notably, FastInsight outperforms Re2 by a larger margin than GAR in the structurally difficult Q2 interval of ACL-OCL, proving its capacity to effectively bridge gaps to oracle nodes even when initial topological proximity is suboptimal.

*Correlation Analysis.* To substantiate these observations, we examine which component of TR captures topological proximity to oracle nodes. Based on Corollary 1, we analyze the correlation between the two components—Recall and MissTR—against the *marginal recall gain* ( $\Delta R = R@100_{total} - R@10_{vs}$  where  $R@100_{total}$  is the recall after complete retrieval and  $R@10_{vs}$  is the recall obtained from initial  $O_{vs}$ ). Here,  $\Delta R$  quantifies the retriever’s success in uncovering remaining undiscovered oracle nodes during graph retrieval.

**Table 6: Correlation coefficient between two metrics and  $\Delta R$ .**

| Methods     | ACL-OCL |             | BSARD-G |             | SciFact-G |             |
|-------------|---------|-------------|---------|-------------|-----------|-------------|
|             | Recall  | MissTR      | Recall  | MissTR      | Recall    | MissTR      |
| GAR         | 0.48    | <b>0.50</b> | 0.46    | <b>0.79</b> | 0.12      | <b>0.65</b> |
| FastInsight | 0.65    | <b>0.66</b> | 0.32    | <b>0.57</b> | 0.10      | <b>0.55</b> |

As shown in Table 6, MissTR consistently exhibits a stronger correlation with  $\Delta R$  than Recall across all datasets and methods. While Recall reflects the success of the initial  $O_{vs}$  retrieval, it shows weak correlation with future discoveries. In contrast, the strong correlation in MissTR suggests that this component effectively captures the topological proximity of the current seed nodes  $N_{sel}$  to undiscovered oracle nodes. Thus, this supports our hypothesis that performance gains in graph-based methods are driven by their ability to exploit such topological structures.

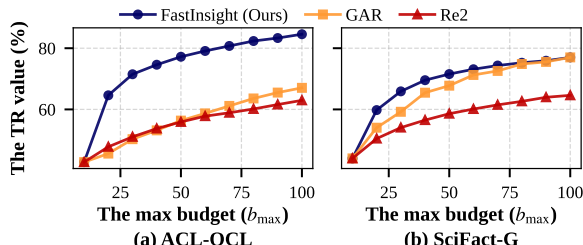


**Figure 6: Evolution of Topological Recall (TR) as a function of retrieval budget ( $b_{max}$ )**

*Evolution of TR in retrieval.* Figure 6 illustrates the evolution of TR as the retrieval budget  $b_{max}$  increases. While all methods exhibit an upward trend, the rise observed in Re2 is largely due to the inherent increase of the Recall term within the decomposed TR equation (Corollary 1). Retrieving a larger volume of nodes naturally increases the likelihood of retrieving oracle nodes, raising the TR score even in the absence of graph traversal. More critically, we

distinguish the trajectories of the graph traversal methods. Unlike GAR, which exhibits a gradual ascent, FastInsight demonstrates a steeper initial rise in TR. This sharp trajectory validates the efficacy of our proposed STeX and GRanker implementations: STeX actively steers node selection towards oracle-rich neighborhoods in the early retrieval stages, while GRanker effectively prioritizes candidates by interpreting their topological context. Consequently, these results provide strong empirical evidence that FastInsight’s mechanisms facilitate truly *insightful retrieval*, securing high topological proximity much faster than competing approaches.

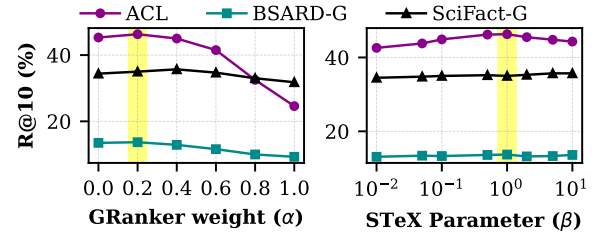


**Figure 7: R@10 sensitivity to GRanker weight (left) and STeX parameter (right).** Yellow bands mark the default values.

**5.3.2 Hyperparameter sensitivity.** Figure 7 illustrates the sensitivity of FastInsight’s R@10 performance to variations in hyperparameters  $\alpha$  and  $\beta$  across three datasets. The results demonstrate that the model achieves consistently high performance across all datasets at our chosen settings of  $\alpha = 0.2$  and  $\beta = 1$ , thereby justifying our parameter selection. Conversely, we observe a degradation in performance when  $\alpha$  approaches 0 (i.e., relying solely on  $O_m$  rather than  $O_{gm}$ ) or when  $\beta$  tends toward extreme values of 0 or  $\infty$  (i.e., using only  $O_{vs}$  or  $O_{gs}$  instead of  $O_{vgs}$ ). These findings demonstrate the contribution of both GRanker and STeX to the overall effectiveness of our proposed method.

## 6 Related Works

Recently proposed retrieval–LLM interleaving methods [27, 30, 32, 37, 39], while effective for problems that go beyond single-step retrieval, rely on frequent LLM invocations, which incur substantial computational overhead and latency, making them impractical for Graph RAG on corpus graphs. Several recent graph retrieval methods aim to conduct effective retrieval by combining two or more operators from  $\{O_{vs}, O_{gs}, O_m\}$  [7, 15, 17, 25]. However, these methods fundamentally adopt on a sequential composition of operators and therefore, inherit the limitations of operators—the topology-blindness of  $O_m$  and the semantic-blindness of  $O_{gs}$ . Moreover, we observe that existing *fusion* approaches, such as G-Retriever [19], can be formally expressed as a composition of our proposed operators  $\{O_{vs}, O_{gs}, O_m\}$ . Specifically, Examples 2 and 4 demonstrate how the PPR algorithm in HippoRAG 2 [17] and G-Retriever [19] are represented within our taxonomy, respectively.

**Example 4 (G-Retriever).** The retrieval in G-Retriever [19] comprises two stages: (1) Vector-Edge Retrieval ( $O_{vs}$ ) and (2) PCST-based subgraph construction ( $O_{gs}$ ), as detailed below:

- (1) *Vector-Edge Retrieval ( $O_{vs}$ ):* It retrieves the top- $k$   $N_{sub} \subset N$  and  $E_{sub} \subset E$  via vector similarity. For the node and edge at rank  $i$ , we assign rank-based prizes  $k - i$  to initialize  $H_{seed}$ .

(2) *PCST Construction ( $O_{\text{gs}}$ ): The operator selects the final subgraph  $\mathcal{N}_{\text{ret}}$  and  $\mathcal{E}_{\text{ret}}$  by optimizing the PCST ranking function:*

$$\mathcal{R}_{\text{PCST}}(\mathcal{N}_{\text{ret}}, \mathcal{E}_{\text{ret}}) = \sum_{n \in \mathcal{N}_{\text{ret}}} p(n) + \sum_{e \in \mathcal{E}_{\text{ret}}} p(e) - c(\mathcal{N}_{\text{ret}}, \mathcal{E}_{\text{ret}})$$

Here,  $p(n)$  and  $p(e)$  correspond to the values in  $\mathbf{H}_{\text{seed}}$ , and  $c(\mathcal{N}_{\text{ret}}, \mathcal{E}_{\text{ret}})$  only depends on  $\mathcal{E}$ .

## 7 Conclusion

In this paper, we presented **FastInsight**, a novel graph retrieval method designed to enable time-efficient and insightful retrieval for Graph RAG on corpus graphs. Specifically, we identify the limitations of existing retrieval operations and overcome them by interleaving two novel fusion operators: **the Graph-based Reranker (GRanker)** for  $O_{\text{gm}}$  and **Semantic-Topological expansion (STE}X** for  $O_{\text{vgs}}$ . Extensive experiments across five corpus graph datasets demonstrate that FastInsight outperforms state-of-the-art baselines by an average of **+9.9% in R@10 and +9.1% in nDCG@10**. Furthermore, compared to conventional LLM interleaving methods, our approach achieves a significant Pareto improvement, **reducing query processing time by 42–58% while simultaneously improving R@10 by 11.7%**.

## References

- [1] Seonho An, Young-Yik Rhim, and Min-Soo Kim. 2025. GReX: A Graph Neural Network-Based Rerank-then-Expand Method for Detecting Conflicts Among Legal Articles in Korean Criminal Law. In *Proceedings of the Natural Legal Language Processing Workshop 2025*, Nikolaos Aletras, Ilias Chalkidis, Leslie Barrett, Cătălina Goanță, Daniel Preotiu-Pietro, and Gerasimos Spanakis (Eds.). Association for Computational Linguistics, Suzhou, China, 408–423. doi:10.18653/v1/2025.nlpl-1.30
- [2] Tu Ao, Yanhua Yu, Yuling Wang, Yang Deng, Zirui Guo, Liang Pang, Pinghui Wang, Tat-Seng Chua, Xiao Zhang, and Zhen Cai. 2025. Lightprof: A light-weight reasoning framework for large language model on knowledge graph. In *Proceedings of the AAAI Conference on Artificial Intelligence*, Vol. 39. 23424–23432.
- [3] Akari Asai, Zeqiu Wu, Yizhong Wang, Avirup Sil, and Hannaneh Hajishirzi. 2024. Self-rag: Learning to retrieve, generate, and critique through self-reflection. (2024).
- [4] Vera Boteva, Demian Gholipour Ghalandari, Artem Sokolov, and Stefan Riezler. 2016. A Full-Text Learning to Rank Dataset for Medical Information Retrieval. In *ECIR (Lecture Notes in Computer Science, Vol. 9626)*, Nicola Ferro, Fabio Crestani, Marie-Francine Moens, Josiane Mothe, Fabrizio Silvestri, Giorgio Maria Di Nunzio, Claudia Hauff, and Gianmaria Silvello (Eds.). Springer, 716–722. <http://dblp.uni-trier.de/db/conf/ecir/ecir2016.html#BotevaGSR16>
- [5] Jake D Brutlag, Hilary Hutchinson, and Maria Stone. 2008. User preference and search engine latency. *JSM Proceedings, Quality and Productivity Research Section* (2008).
- [6] RONALD S. BURT. 1992. *Structural Holes: The Social Structure of Competition*. Harvard University Press. <http://www.jstor.org/stable/j.ctv1kz4h78>
- [7] Boyu Chen, Zirui Guo, Zidan Yang, Yuluo Chen, Junze Chen, Zhenghao Liu, Chuan Shi, and Cheng Yang. 2025. PathRAG: Pruning Graph-based Retrieval Augmented Generation with Relational Paths. arXiv:2502.14902 [cs.CL] <https://arxiv.org/abs/2502.14902>
- [8] Huan Chen, Gareth JF Jones, and Rob Brennan. 2024. An Examination of Embedding Methods for Entity Comparison in Text-Rich Knowledge Graphs. In *Proceedings of the Proceedings of the 32nd Irish Conference on Artificial Intelligence and Cognitive Science (AICS 2024). CEUR Workshop Proceedings*.
- [9] Thomas Cook, Richard Osuagwu, Liman Tsatiashvili, Vrynsia Vrynsia, Koustav Ghosal, Maraim Masoud, and Riccardo Mattivi. 2025. Retrieval Augmented Generation (RAG) for Fintech: Agentic Design and Evaluation. *arXiv preprint arXiv:2510.25518* (2025).
- [10] Darren Edge, Ha Trinh, Newman Cheng, Joshua Bradley, Alex Chao, Apurva Mody, Steven Troutt, Dasha Metropolitansky, Robert Osazuwa Ness, and Jonathan Larson. 2024. From local to global: A graph rag approach to query-focused summarization. *arXiv preprint arXiv:2404.16130* (2024).
- [11] Thibault Formal, Benjamin Piwowarski, and Stéphane Clinchant. 2021. SPLADE: Sparse lexical and expansion model for first stage ranking. In *Proceedings of the 44th International ACM SIGIR Conference on Research and Development in Information Retrieval*. 2288–2292.
- [12] Luyu Gao, Xueguang Ma, Jimmy Lin, and Jamie Callan. 2023. Precise Zero-Shot Dense Retrieval without Relevance Labels. In *Proceedings of the 61st Annual Meeting of the Association for Computational Linguistics (Volume 1: Long Papers)*, Anna Rogers, Jordan Boyd-Graber, and Naoaki Okazaki (Eds.). Association for Computational Linguistics, Toronto, Canada, 1762–1777. doi:10.18653/v1/2023.acl-long.99
- [13] Yunfan Gao, Yun Xiong, Xinyu Gao, Kangxiang Jia, Jinliu Pan, Yuxi Bi, Yixin Dai, Jiawei Sun, Haofen Wang, and Haofen Wang. 2023. Retrieval-augmented generation for large language models: A survey. *arXiv preprint arXiv:2312.10997* 2, 1 (2023).
- [14] Mark S Granovetter. 1973. The strength of weak ties. *American journal of sociology* 78, 6 (1973), 1360–1380.
- [15] Zirui Guo, Lianghao Xia, Yanhua Yu, Tu Ao, and Chao Huang. 2025. LightRAG: Simple and Fast Retrieval-Augmented Generation. arXiv:2410.05779 [cs.IR] <https://arxiv.org/abs/2410.05779>
- [16] Zirui Guo, Lianghao Xia, Yanhua Yu, Tu Ao, and Chao Huang. 2025. LightRAG: Simple and Fast Retrieval-Augmented Generation. In *Findings of the Association for Computational Linguistics: EMNLP 2025*, Christos Christodoulopoulos, Tanmoy Chakrabarty, Carolyn Rose, and Violet Peng (Eds.). Association for Computational Linguistics, Suzhou, China, 10746–10761. doi:10.18653/v1/2025.findings-emnlp.568
- [17] Bernal Jiménez Gutiérrez, Yiheng Shu, Weijian Qi, Sizhe Zhou, and Yu Su. 2025. From RAG to Memory: Non-Parametric Continual Learning for Large Language Models. In *Forty-second International Conference on Machine Learning*. <https://openreview.net/forum?id=LWH8yn4HS2>
- [18] Haoyu Han, Yu Wang, Harry Shomer, Kai Guo, Jiayuan Ding, Yongjia Lei, Mahantesh Halappanavar, Ryan A Rossi, Subhabrata Mukherjee, Xianfeng Tang, et al. 2024. Retrieval-augmented generation with graphs (graphrag). *arXiv preprint arXiv:2501.00309* (2024).
- [19] Xiaoxin He, Yijun Tian, Yifei Sun, Nitesh Chawla, Thomas Laurent, Yann LeCun, Xavier Bresson, and Bryan Hooi. 2024. G-retriever: Retrieval-augmented generation for textual graph understanding and question answering. *Advances in Neural Information Processing Systems* 37 (2024), 132876–132907.
- [20] Yuntong Hu, Zhihan Lei, Zheng Zhang, Bo Pan, Chen Ling, and Liang Zhao. 2025. GRAG: Graph Retrieval-Augmented Generation. In *Findings of the Association for Computational Linguistics: NAACL 2025*, Luis Chirizzo, Alan Ritter, and Lu Wang (Eds.). Association for Computational Linguistics, Albuquerque, New Mexico, 4145–4157. doi:10.18653/v1/2025.findings-naacl.232
- [21] Yiqian Huang, Shiqi Zhang, and Xiaokui Xiao. 2025. Ket-rag: A cost-efficient multi-granular indexing framework for graph-rag. In *Proceedings of the 31st ACM SIGKDD Conference on Knowledge Discovery and Data Mining* V. 2. 1003–1012.
- [22] Gautier Izacard, Mathilde Caron, Lucas Hosseini, Sebastian Riedel, Piotr Bojanowski, Armand Joulin, and Edouard Grave. 2022. Unsupervised Dense Information Retrieval with Contrastive Learning. *Transactions on Machine Learning Research* (2022). <https://openreview.net/forum?id=jKN1pXi7b0>
- [23] Soyeong Jeong, Jinheon Baek, Sukmin Cho, Sung Ju Hwang, and Jong Park. 2024. Adaptive-RAG: Learning to Adapt Retrieval-Augmented Large Language Models through Question Complexity. In *Proceedings of the 2024 Conference of the North American Chapter of the Association for Computational Linguistics: Human Language Technologies (Volume 1: Long Papers)*, Kevin Duh, Helena Gomez, and Steven Bethard (Eds.). Association for Computational Linguistics, Mexico City, Mexico, 7036–7050. doi:10.18653/v1/2024.naacl-long.389
- [24] Xinke Jiang, Ruizhe Zhang, Yongxin Xu, Rihong Qiu, Yue Fang, Zhiyuan Wang, Jinyi Tang, Hongxin Ding, Xu Chu, Junfeng Zhao, and Yasha Wang. 2024. HyKGE: A Hypothesis Knowledge Graph Enhanced Framework for Accurate and Reliable Medical LLMs Responses. arXiv:2312.15883 [cs.CL] <https://arxiv.org/abs/2312.15883>
- [25] Bernal Jimenez Gutierrez, Yiheng Shu, Yu Gu, Michihiro Yasunaga, and Yu Su. 2024. Hipporag: Neurobiologically inspired long-term memory for large language models. *Advances in Neural Information Processing Systems* 37 (2024), 59532–59569.
- [26] Kaeun Kim, Ghazal Shams, and Kawon Kim. 2025. From Seconds to Sentiments: Differential Effects of Chatbot Response Latency on Customer Evaluations. *International Journal of Human–Computer Interaction* (2025), 1–17.
- [27] Myeonghwa Lee, Seonho An, and Min-Soo Kim. 2024. PlanRAG: A Plan-then-Retrieval Augmented Generation for Generative Large Language Models as Decision Makers. In *Proceedings of the 2024 Conference of the North American Chapter of the Association for Computational Linguistics: Human Language Technologies (Volume 1: Long Papers)*, Kevin Duh, Helena Gomez, and Steven Bethard (Eds.). Association for Computational Linguistics, Mexico City, Mexico, 6537–6555. doi:10.18653/v1/2024.naacl-long.364
- [28] Mufei Li, Siqi Miao, and Pan Li. 2025. Simple is Effective: The Roles of Graphs and Large Language Models in Knowledge-Graph-Based Retrieval-Augmented Generation. In *The Thirteenth International Conference on Learning Representations*. <https://openreview.net/forum?id=JvkuZZ04O7>
- [29] Antoine Louis and Gerasimos Spanakis. 2022. A Statutory Article Retrieval Dataset in French. In *Proceedings of the 60th Annual Meeting of the Association for Computational Linguistics (Volume 1: Long Papers)*, Smaranda Muresan, Preslav

- Nakov, and Aline Villavicencio (Eds.). Association for Computational Linguistics, Dublin, Ireland, 6789–6803. doi:10.18653/v1/2022.acl-long.468
- [30] Shengjie Ma, Chengjin Xu, Xuhui Jiang, Muzhi Li, Huaren Qu, Cehao Yang, Jiaxin Mao, and Jian Guo. 2025. Think-on-Graph 2.0: Deep and Faithful Large Language Model Reasoning with Knowledge-guided Retrieval Augmented Generation. In *The Thirteenth International Conference on Learning Representations*. <https://openreview.net/forum?id=oFBu7qaZpS>
- [31] Sean MacAvaney, Nicola Tonello, and Craig Macdonald. 2022. Adaptive Re-Ranking with a Corpus Graph. In *Proceedings of the 31st ACM International Conference on Information & Knowledge Management* (Atlanta, GA, USA) (CIKM '22). Association for Computing Machinery, New York, NY, USA, 1491–1500. doi:10.1145/3511808.3557231
- [32] Costas Mavromatis and George Karypis. 2024. Gnn-rag: Graph neural retrieval for large language model reasoning. *arXiv preprint arXiv:2405.20139* (2024).
- [33] Hongjin Qian, Zheng Liu, Peitian Zhang, Kelong Mao, Defu Lian, Zhicheng Dou, and Tiejun Huang. 2025. MemoRAG: Boosting Long Context Processing with Global Memory-Enhanced Retrieval Augmentation. In *Proceedings of the ACM on Web Conference 2025* (Sydney NSW, Australia) (WWW '25). Association for Computing Machinery, New York, NY, USA, 2366–2377. doi:10.1145/3696410.3714805
- [34] Manddeep Rathee, Sean MacAvaney, and Avishek Anand. 2025. Guiding retrieval using llm-based listwise rankers. In *European Conference on Information Retrieval*. Springer, 230–246.
- [35] Shaurya Rohatgi, Yanxia Qin, Benjamin Aw, Niranjana Unnithan, and Min-Yen Kan. 2023. The ACL OCL Corpus: Advancing Open Science in Computational Linguistics. In *Proceedings of the 2023 Conference on Empirical Methods in Natural Language Processing*. Houda Bouamor, Juan Pino, and Kalika Bali (Eds.). Association for Computational Linguistics, Singapore, 10348–10361. doi:10.18653/v1/2023.emnlp-main.640
- [36] Michael Shen, Muhammad Umar, Kiwan Maeng, G. Edward Suh, and Udit Gupta. 2024. Towards Understanding Systems Trade-offs in Retrieval-Augmented Generation Model Inference. *arXiv:2412.11854 [cs.AR]* <https://arxiv.org/abs/2412.11854>
- [37] Jiashuo Sun, Chengjin Xu, Lumingyuan Tang, Saizhuo Wang, Chen Lin, Yeyun Gong, Lionel Ni, Heung-Yeung Shum, and Jian Guo. 2024. Think-on-Graph: Deep and Responsible Reasoning of Large Language Model on Knowledge Graph. In *The Twelfth International Conference on Learning Representations*. <https://openreview.net/forum?id=nnVO1PvbTv>
- [38] Nandan Thakur, Nils Reimers, Andreas Rücklé, Abhishek Srivastava, and Iryna Gurevych. 2021. BEIR: A Heterogeneous Benchmark for Zero-shot Evaluation of Information Retrieval Models. In *Proceedings of the Neural Information Processing Systems Track on Datasets and Benchmarks 1, NeurIPS Datasets and Benchmarks 2021, December 2021, virtual*. Joaquin Vanschoren and Sai-Kit Yeung (Eds.). <https://datasets-benchmarks-proceedings.neurips.cc/paper/2021/hash/65b9eea6e1cc6bb9f0cd2a47751a186f-Abstract-round2.html>
- [39] Harsh Trivedi, Niranjan Balasubramanian, Tushar Khot, and Ashish Sabharwal. 2023. Interleaving Retrieval with Chain-of-Thought Reasoning for Knowledge-Intensive Multi-Step Questions. In *Proceedings of the 61st Annual Meeting of the Association for Computational Linguistics (Volume 1: Long Papers)*. Anna Rogers, Jordan Boyd-Graber, and Naoki Okazaki (Eds.). Association for Computational Linguistics, Toronto, Canada, 10014–10037. doi:10.18653/v1/2023.acl-long.557
- [40] David Wadden, Shanchuan Lin, Kyle Lo, Lucy Lu Wang, Madeleine van Zuylen, Arman Cohan, and Hannaneh Hajishirzi. 2020. Fact or Fiction: Verifying Scientific Claims. In *Proceedings of the 2020 Conference on Empirical Methods in Natural Language Processing (EMNLP)*. Bonnie Webber, Trevor Cohn, Yulan He, and Yang Liu (Eds.). Association for Computational Linguistics, Online, 7534–7550. doi:10.18653/v1/2020.emnlp-main.609
- [41] Jiaosheng Zhang, Ali Maatouk, Jialin Chen, Ngoc Bui, Qianqian Xie, Leandros Tassiulas, Hua Xu, Jie Shao, and Rex Ying. 2025. LitFM: A Retrieval Augmented Structure-aware Foundation Model for Citation Graphs. In *Proceedings of the 31st ACM SIGKDD Conference on Knowledge Discovery and Data Mining V.2* (Toronto ON, Canada) (KDD '25). Association for Computing Machinery, New York, NY, USA, 3728–3739. doi:10.1145/3711896.3737028
- [42] Xiangrong Zhu, Yuxiang Xie, Yi Liu, Yaliang Li, and Wei Hu. 2025. Knowledge Graph-Guided Retrieval Augmented Generation. In *Proceedings of the 2025 Conference of the Nations of the Americas Chapter of the Association for Computational Linguistics: Human Language Technologies (Volume 1: Long Papers)*. Luis Chiruzzo, Alan Ritter, and Lu Wang (Eds.). Association for Computational Linguistics, Albuquerque, New Mexico, 8912–8924. doi:10.18653/v1/2025.naacl-long.449